Cloud Droplet Growth by Collection[1]

E. X BERRY

Desert Research Institute, University of Nevada, Reno

(Manuscript received 28 December 1966, in revised form 30 March 1967)

ABSTRACT

Calculations of cloud droplet growth over the radius range from 4 to 200 μ for collection kernels representing hydrodynamic capture, electric field capture, and geometric sweep-out show that the rate of droplet growth is proportional to the magnitude of the kernel, and the pattern of growth depends upon a derivative of the kernel with respect to droplet size. Below 60 μ a large kernel derivative causes the distribution to spread. Above 60 μ the derivative of each kernel decreases to a common value that causes water to accumulate on large drops. This leads to a self-preserving distribution, similar to Golovin's asymptotic solution, in about 5 min when the liquid water content is 1 gm m^{-3}. The stochastic model produces a growth rate nearly equal to the continuous model but transfers much more water to larger drops.

Nomenclature

t	time
r,r_s	radius of larger (smaller) droplet
p	r/r_s
x,x'	mass of collector (collected) droplet
x_c	$x-x'$, mass that collects x' to form x
x_0	smallest mass to undergo collection
J,J'	computation parameters for x,x'
J_c	computation parameter for x_c
J_0	scale factor for computation parameter
J_d	computation parameter for $x/2$
j	computation parameter equal to sets of mass-multiples
$v(r)$	terminal fall velocity for droplet with radius r
Δv	difference in velocities of two droplets
Y_c	linear collision efficiency
E_c	collision efficiency
$V(x\|x')$	collection kernel of x with respect to x'
$P(x\|x')$	probability that x droplet collects x' droplet during δt
$f\langle q\rangle$	number density function over parameter q
$g\langle q\rangle$	$xf\langle q\rangle$, mass density function over parameter q
$\bar{x}_f$	mean mass of number density function
$\bar{x}_g$	mean mass of mass density function
$\sigma_g(x)$	standard deviation in mass of mass density function
$\sigma_f(r)$	standard deviation in radius of number density function
$M\langle\ln r_s\rangle$	density function of water mass captured by 100-μ drop
s	$x/\bar{x}_{f0}$
N	total number of droplets m^{-3} of air
L	total mass of droplets m^{-3} of air
Z	radar reflectivity
b	a constant in the collection kernel
τ	$1-\exp(-bLt)$, transformed time used in analytic solution
I_1	modified Bessell function of order 1
ρ	density of water
g_m	asymptotic maximum of $g\langle\ln r\rangle$
x_m	asymptotic mode of $g\langle\ln r\rangle$

[1] Work supported by NSF Grant GA-463.

1. The warm rain process

The numerical calculations of Howell (1949), Mordy (1959), and Neiburger and Chien (1960) show that droplet growth by condensation produces only a relatively narrow distribution of small droplets during the hour or two lifetime of a typical cumulus cloud. The broadening of this distribution to include some larger droplets or ice particles can occur either by collision and coalescence or by the Bergeron process, whereby ice crystals gather by vapor diffusion the water from surrounding supercooled droplets. Precipitation may result after coalescence is "initiated" between the large and small particles, water or ice (Byers, 1965).

The occurence of collision and subsequent coalescence among cloud particles is called "collection." Observations of rain from tropical cumulus whose tops had temperatures above 0C (Heywood, 1940; Mordy and Eber, 1954; Byers and Hall, 1955) has caused droplet collection to be labeled the "warm rain" process (Squires, 1955). But its importance extends to colder clouds. Braham (1964) found that droplets in supercooled summer cumulus over the central United States develop by the warm rain process before they freeze.

2. Two collection models

To describe how a distribution of particles changes with collection, we consider every possible combination of particles that can coalesce, the probability of each

coalescence, and the change in these probabilities after each coalescence. The resulting particle growth is a stochastic process; we call this model the "stochastic mode." It will be formulated later.

The complexity of the collection equation for cloud droplet growth led Langmuir (1948) and Bowen (1950) to reduce the problem to its simplest elements. They postulated that the droplet distribution consists of two discrete sizes: small droplets, of which there are many, and large drops, of which there are few. The small droplets, with constant size and number, are visualized as filling space with a uniform density of water which the large drops sweep out continuously as they fall. All large drops grow at the same continuous rate; we call this model the "continuous model" (Fig. 1A).

The stochastic model assigns to each potential coalescence a probability that it will occur in a given time interval. During this time only a fraction (equal to the probability) of many similar potential coalescences actually takes place, and one size of large drops becomes two sizes of large drops. During the next time interval a fraction of the drops from each large size collects small droplets and spreads the distribution further. A small portion of the large drops grows much faster than the rest (Fig. 1B). This probabilistic nature of collection results from the random locations of the smaller droplets and the consequent probability that one lies in the volume to be swept out by a larger drop.

A complete formulation of collection would include the fluctuation in the number of droplets of each size in a specified volume of air. Scott (1967) has shown that the fluctuation in cloud droplet concentrations is small enough that their mean number is a good approximation in coalescence studies.

The stochastic model focuses attention upon the change in the value of the density function representing the droplets. The continuous model directs attention to the size of the larger drops. This simplification is possible for a small number of sizes of larger drops but not for a broad distribution of droplets.

Telford (1955) used a discrete size distribution to demonstrate mathematically that the stochastic model produces a few large droplets much faster than the continuous model. He did not solve the stochastic growth equation for a broad distribution, but did show that the stochastic model could better explain the observed rapid formation of large drops in warm clouds.

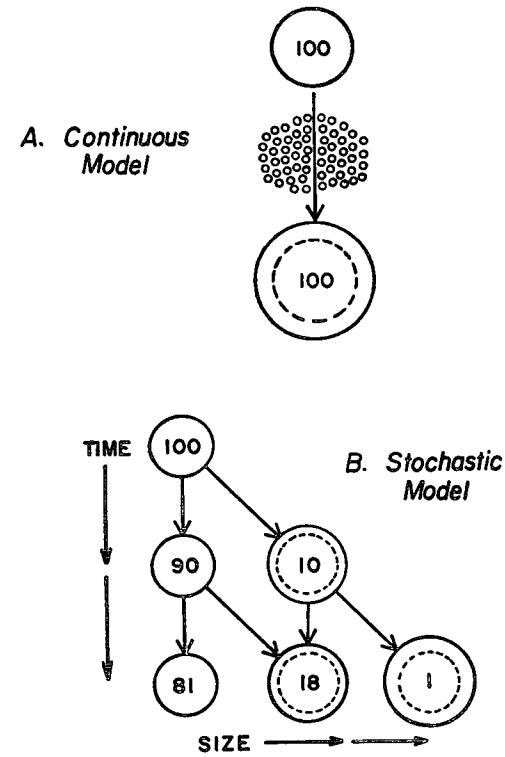

FIG. 1. The continuous and stochastic models. A. The continuous model assumes that small droplets are swept out as if their water were distributed uniformly in space. 100 large drops grow at the same rate and become 100 similar larger drops. B. The stochastic model assumes that, say, 1 in 10 of 100 large droplets will collect a small droplet during a given time, and then 1 in 10 of each large size will collect a smaller droplet. Large droplets then grow at different rates. The distribution spreads.

3. Density function nomenclature

There are two types of functions regularly used in science: analytic functions and density functions. They have different properties and different meanings, and they transform differently.[2] They should have different nomenclature so that they can readily be distinguished.

Since the conclusions reached in this paper derive from the transformation to uncommon density functions, it is essential to show explicitly how they are related to the more common ones. While it is not absolutely necessary, it is extremely convenient to introduce a special symbol to represent a density function.

Therefore, we define

$$f\langle q\rangle = f_q(q), \tag{1}$$

where q is the independent variable and $f_q(q)$ is, according to the terminology in the *Glossary of Meteorology* (Huschke, 1959), the "probability density function" or, simply, "density function." Henceforth, we shall use ⟨angle brackets⟩ to enclose the argument of a density function and (parentheses) for an analytic function.

As a "probability density function," $f\langle q\rangle$ has the

[2] They are distinguished in tensor terminology by the "weight" assigned to the "relative scalar." A relative scalar of weight zero is an "absolute scalar" or analytic function. A relative scalar of weight one is a "scalar density" or density function (Sokolnikoff, 1951).

following properties:

$$\left.\begin{aligned} &f\langle q\rangle \geq 0 \\ &\int_0^\infty f\langle q\rangle dq = 1 \\ &\int_a^b f\langle q\rangle dq = P[a<q<b] \end{aligned}\right\}, \tag{2}$$

where the last equation means that the area under the curve between any two values of q is equal to the probability upon sampling the population of finding a member having the parameter q between these values, or, considering the population as a whole, the area is equal to that proportion of the total number of the population whose members have q between a and b.

In the more general sense, as a "density function," the normalization of $f\langle q\rangle$ may be disregarded and the area under the curve set equal to the total number of those members in the population that have q between a and b. In many physical applications when the population is well defined, this more general interpretation of $f\langle q\rangle$ is more useful since it shows directly any change of the total population. It is also an interpretation that readily lends itself to the transformation of $f\langle q\rangle$ to other density functions. The units of $f\langle q\rangle$ are always "the number of objects per unit of its argument," and a plot of $f\langle q\rangle$ as a true density function, such that the area under the curve has meaning,[3] must use these units as well as a linear scale of q.

The transformation of the independent variable of a density function from q to p, where $q=\phi(p)$, gives a new density function $f\langle p\rangle$. From the definition of a density function the transformation is subject to the constraint, which defines $f\langle p\rangle$,

$$\int_a^b f\langle p\rangle dp = \int_{\phi(a)}^{\phi(b)} f\langle q\rangle dq, \tag{3}$$

or, more simply,

$$f\langle p\rangle = \phi'(p) f\langle \phi(p)\rangle. \tag{4}$$

Thus, $f\langle p\rangle$ and $f\langle q\rangle$ represent the same set of particles but they are not the same function. In order for the area under their curves to have meaning each must be plotted over a linear scale of its argument. Density functions are related by the Jacobian of the coordinate transformation. By contrast, change of the independent variable of an analytic function does not involve the Jacobian,

$$h(p) = f[\phi(p)].$$

[3] A density function $f\langle q\rangle$ may be designated by dF/dq, where

$$F(q) = \int_0^q f\langle q\rangle dq$$

is the cumulative distribution function or, simply, distribution function. This is not a convenient form and it does not reduce the desirability of having a distinct notation.

The transformation of a density function from one argument to another is simplest when both arguments are unitless indices. This is essential when the transformation is logarithmic since the logarithm can be taken only of a unitless number. Let x_1 and r_1 be the basic units of mass and radius (and assume that the objects are spherical with equal density). Then, according to (4), using unitless parameters, the relationships of the density function over mass to those over radius, the logarithm of mass, and the logarithm of radius are:

$$\left.\begin{aligned} &f\langle x/x_1\rangle = (1/3)(r/r_1)(x_1/x) f\langle r/r_1\rangle \\ &f\langle x/x_1\rangle = (x_1/x) f\langle \ln(x/x_1)\rangle \\ &f\langle x/x_1\rangle = (1/3)(x_1/x) f\langle \ln(r/r_1)\rangle \end{aligned}\right\}. \tag{5}$$

When x_1 and r_1 are set equal to one unit, the relations take on the more familiar forms,

$$\left.\begin{aligned} &f\langle x\rangle = (1/3)(r/x) f\langle r\rangle \\ &f\langle x\rangle = (1/x) f\langle \ln x\rangle \\ &f\langle x\rangle = (1/3)(1/x) f\langle \ln r\rangle \end{aligned}\right\}. \tag{6}$$

The second type of transformation is the change of a density function to one of its moments. An example is the "*mass* density function,"

$$g(q) = x f\langle q\rangle. \tag{7}$$

Its units are "the mass of objects per unit of its argument." The area under the curve $g\langle q\rangle$ between any two values of q is equal to the total *mass* of those members of the population that have q between these two values. The mass density function, like the density function, can have as its argument any parameter related to q. The transformations of $g\langle q\rangle$ are given by replacing f by g in (4), (5) and (6).

The values of a density function of $f\langle q_i\rangle$ and those of a histogram $N\langle q_i\rangle$ are easily compared by specifying the histogram unit h in the units of the density function q.

Then,

$$f\langle q_i\rangle = (1/h)\int_{q_i-h/2}^{q_i+h/2} f\langle q\rangle dq = N\langle q_i\rangle/h \tag{8}$$

is the value of $f\langle q\rangle$ at $q=q_i$ when $N\langle q_i\rangle$ objects have been counted having $(q_i-h/2)<q<(q_i+h/2)$.

Two deviations have occasionally been made in the method of plotting density functions. The first has been the use of a logarithmic scale for the ordinate, and the second has been the use of a logarithmic scale for the abscissa when the density function has units of, say, "number per micron radius." Both of these uses do have the advantage of amplifying one end or the other of the scale, but have also the great disadvantage of losing the meaning of the area under the curve. The desired advantages can almost always be obtained, without losing the meaning of the area under the curve, by a

well-chosen density function. One purpose of a density function is to display information.

4. The formulation of stochastic collection

Let the density function $f\langle x\rangle$ be defined such that $f\langle x\rangle dx$ is the mean number of droplets of mass x to $x+dx$ in a unit volume of air. Let the expression "x-droplet" mean a droplet of mass x. Also define the collection kernel $V(x|x')$ as the rate at which the volume within which an x'-droplet will be captured is swept out by an x-droplet. This volume rate is a function of the size of both particles concerned and is related to the linear collision efficiency Y_c used by Shafrir and Neiburger (1963) and to the collision efficiency E_c used by Plumlee and Semonin (1965) as follows:

$$V(r|r_s)=\pi r^2 Y_c(r|r_s)^2\Delta v(r,r_s), \tag{9a}$$

$$=\pi(r+r_s)^2 E_c(r|r_s)\Delta v(r,r_s), \tag{9b}$$

where r,r_s is the radius of the larger (smaller) droplet, and Δv the difference in velocities. For lack of information to the contrary we assume that every collision results in a coalescence.

The probability that a particular x-droplet will collect an x'-droplet during the time interval δt is

$$P(x|x')=\delta t V(x|x')f\langle x'\rangle dx', \tag{10}$$

where, in order that $P(x|x')$ be a true probability measure, δt is small enough that the probability of finding two x'-droplets in the volume $\delta t\cdot V(x|x')$ is negligible. In the time δt and in a unit volume of air the mean number of x-droplets that collect x'-droplets is

$$f\langle x\rangle dx P(x|x')=f\langle x\rangle dx\delta t V(x|x')f\langle x'\rangle dx. \tag{11}$$

The total change $\delta f\langle x\rangle dx$ in the number of x-droplets is due to two effects: all collections which form an x-droplet, and all collections which destroy an x-droplet. This total change is accounted for by two integrals. By letting $\delta t\to 0$, we find the mean rate of change of the density function at the mass x to be

$$\partial f\langle x\rangle/\partial t=\int_{x_0}^{x/2} dx' f\langle x_c\rangle V(x_c|x')f\langle x'\rangle - \int_{x_0}^{\infty} dx' f\langle x\rangle V(x|x')f\langle x'\rangle, \tag{12}$$

where $x_c=x-x'$.

This is the stochastic collection equation. The partial derivative[4] means that we are looking at a change in the density function at a constant x.

[4] A total derivative would imply that we are looking at the change in the density function while following the x of a given group of particles, which is absurd because particles lose their identity upon coalescence: two are destroyed, one is created. Certainly, in the case of continuous growth where only large and small particles exist, the "identity" may be attached to the larger. Then attention may be focused upon the mass of the larger particles themselves, as mentioned above.

The lower limit x_0 of the integrals is the smallest mass for which collection is considered. The simplicity of the formulation is due to mass conservation during coalescence.

5. Solutions to the stochastic equation

The stochastic collection equation (12) has been used by investigators of aerosol coagulation and is given in the *Handbook on Aerosols* (1950). Melzak (1957) demonstrated the existence and uniqueness of its solutions and added a term describing particle breakup. Chandrasekhar (1943) examined the formulation of the collection problem as applied to colloidal particles.

The complexity of the collection kernel for many practical applications of (12) makes numerical solutions necessary. Zebel (1958) calculated the coagulation of aerosols numerically (but did not describe his methods). Hidy (1965) used the formulation of collection by Smoluchowksi (1916) in terms of discrete mass intervals, rather than with integrals and a density function, as a basis of his numerical integrations of aerosol coagulation.

A major breakthrough in solving the stochastic collection equation for cloud droplets was the analytic solution of Golovin (1963) for a collection kernel proportional to the sum of the masses of the droplets. This kernel, he noticed, is similar to the kernel for the larger cloud droplets. Following this lead, Scott (1965) extended the range of analytic solutions to a wider variety of initial density functions and to two other kernels: the product of droplet masses and a constant.

Twomey's (1964) numerical integration of the stochastic collection equation used an initial density function that represented a typical droplet spectrum produced by condensation. Whereas Hidy had divided his distribution into equal mass intervals, Twomey chose to express the equation in equal radius intervals.

An inherent difficulty in the numerical solution of cloud droplet collection is the wide range of sizes that must be considered (say from 1 to 100 μ), coupled with the detail needed to describe the distribution at the small sizes and the practical limitation on data points in a numerical computation. Equal divisions in particle mass, although giving the simplest formulation of the problem, severely restrict the range of particle sizes that can be considered numerically. Equal divisions in particle radius provide a slightly more detailed look at the small sizes but necessitate a subsidiary calculation of one size and density function for each pair of droplets that coalesce. Unequal size intervals bring additional numerical difficulties.

Twomey's calculations reinforced Telford's earlier conclusions and showed that larger droplets are produced even faster when the integral form of the stochastic collection equation is used. This increase is due to the use of a smooth rather than discrete distribution function, to the time derivative of the density function

in (12) rather than a time step (which means that the time interval in Fig. 1B has approached zero), and to the use of a collection kernel that increases with collector size (which corresponds to increasing the collection probability for the largest drops in the second step in Fig. 1B from 1 in 10 to, say, 2 in 10). All these were used by Twomey but none by Telford.

In a subsequent paper Twomey (1966) extended his model to include the radius range of 1 to 1000 μ by using an irregular spacing of intervals: 1 μ up to 20 μ, 1.5 μ up to 32 μ, 2 μ to 40 μ, etc., and 10 μ above 100 μ. He recognized that greater spacing must be used at larger radii in order to include a reasonable number of drops in the counting interval and to allow a wide total size range in a reasonable number of points; but his method introduces unnecessary numerical difficulties that may have prompted his crucial assumption that the continuous growth model is accurate for droplets with radii greater than 50 μ. He concluded that varying the relative dispersion of the initial spectrum, while keeping the total liquid water content constant, made no great difference in the evolution of larger droplets.

Bartlett (1966) did not use the stochastic collection equation but assembled new droplets by the addition of categories and an interpolation scheme designed to preserve liquid water. His calculation with size intervals of 1 μ extended only to 40 μ. Droplets larger than this he assumed "to leave the parcel of air under consideration and to eventually fall out of the cloud as precipitation."

The present paper contains results of numerical calculations of droplet growth according to the stochastic collection model over the radius range 4–200 μ which show that the growth of a 50-μ droplet to a raindrop is not described by the continuous model and, consequently, the stochastic process above 50 μ produces a droplet distribution similar to Golovin's (1963) asymptotic solution in about 5 min when the liquid water content is 1 gm m^{-3}. A logarithmic scale for droplet size accomplishes the necessary "stretching" of radius categories and simplifies the numerical procedures.[5]

6. The cloud model

We assume for a cloud model an infinitely high cylinder immersed in a homogeneous, isotropic distribution of cloud droplets in air. The air is still, and as each droplet falls at terminal velocity, it has a probability that within the next time interval it will collide and coalesce with another droplet. This occurrence among a large number of droplets changes the size distribution through the formation of larger and fewer droplets. This model neglects the variations in the droplet distribution with height, but is representative of an isotropic column in a real cloud whose height exceeds the mean distance that the droplets fall through the air during the computation.

[5] The resulting program is not excessively time or space consuming. It has run at 6 times real-time on a relatively small and slow computer, a CDC 1604 (Berry, 1965).

7. Reformulation for numerical solution

To achieve a satisfactory set of points to present the density function, we transform the mass to a logarithmic scale in terms of a "computation parameter" J by setting

$$x(J)=x_0\exp[3(J-1)/J_0], \tag{13}$$

where x_0 is the smallest mass considered, J_0 is an adjustable scale factor that fixes the desired data points at integer values of J, and the factor 3 is included to make the radius ($\sim x^{1/3}$) take a simple form. Unity is subtracted from J so J will be non-zero and thus can be used directly as a subscript in Fortran.

This transformation results in a new density function and a new collection equation, i.e.,

$$f\langle J\rangle=3(x/J_0)f\langle x\rangle, \tag{14}$$

$$\partial f\langle J\rangle/\partial t=\int_1^{J_d} dJ'(x/x_c)j\langle J_c\rangle V(J_c|J')f\langle J'\rangle - \int_1^{\infty} dJ' f\langle J\rangle V(J|J')f\langle J'\rangle, \tag{15}$$

$$J_d=J-(J_0/3)\ln 2, \tag{16}$$

$$J_c=1+(J_0/3)\ln[1-\exp\{3(J-J')/J_0\}]. \tag{17}$$

The collector parameter $J_c(J-J')$ is a vector, easily stored.

We make the upper limit J_d of the first integral in (15) coincide with an integer value of J by setting

$$(J_0/3)\ln 2=j, \tag{18}$$

where j is an integer greater than zero. This simultaneously sets the data points J to j interlaced sets of mass-multiples by reducing (13) to

$$x(J)=x_0 2^{(J-1)/j}. \tag{19}$$

The calculations shown herein used $j=2$, which was found by trial to give sufficient accuracy for the chosen conditions. $f\langle J_c\rangle$ was calculated at each integration step by a Langrangian 3-point interpolation on $f\langle J\rangle$.

The smallness of the density function at larger radii requires a decision between calling the function identically zero or a step above zero in the computer. A test calculation was tried both ways and no difference resulted. Another test was made using a much higher lower limit than required by the machine, so that the ratio of maximum $f\langle J\rangle$ to minimum $f\langle J\rangle$ was 10^{17}. This difference also did not affect the result. The computations shown herein used 10^{38} for this ratio.

8. Checks on the accuracy of the numerical computations

The accuracy of the numerical computations was subject to five independent safeguards:

1) The density function $f\langle J\rangle$ was represented over the radius range from 3.94 to 400 μ (in 41 points). Although results are shown here only to 200 μ, the effect of droplets up to 400 μ is included in the computations. The calculations were stopped when $f\langle J\rangle$ at 400 μ became significantly large.

2) The total quantity of liquid water was periodically calculated from the density function and the computations stopped if its error exceeded 5%. Most of the results shown here deviated less than 2% from the original water content.

3) The standard check of halving the time step produced negligible change. (The time steps used in these calculations were 5 and 10 sec.)

4) The known analytic solution of Golovin (1963) was evaluated and compared with the numerical calculation having the same kernel and initial density function (see Fig. 3).

5) Twelve separate kernels were used which deviated only slightly from one another and which progressively bridged the gap from Golovin's kernel to that for hydrodynamic capture.

9. The initial density function

Droplet growth is displayed by the droplet mass density function with respect to the natural logarithm of the droplet radius, designated $g\langle \ln r\rangle$. It is related to $f\langle \ln r\rangle$, $f\langle x\rangle$and $f\langle J\rangle$, according to (4) and (7), as follows:

$$g\langle \ln r\rangle = xf\langle \ln r\rangle = 3x^2 f\langle x\rangle = xJ_0 f\langle J\rangle. \quad (20)$$

The units of $g\langle \ln r\rangle$ are mass of droplets per unit of $\ln r$. This density function tells how the liquid water mass is distributed over droplets of various radii, when the radius is plotted on a logarithmic scale. The area under the curve between any two values of the radius will be equal to the liquid water mass per cubic meter of air contained by droplets having radii between these same two values.

The mass density function with respect to $\ln r$ was chosen for the display of the numerical results because 1) the liquid water mass is fundamental to reasoning in cloud physics, 2) water mass is conserved in collection, hence the area under the mass curve will remain constant, 3) it provides a good criterion for deciding when a quantity is negligible, 4) the $\ln r$ scale shows the necessary detail at the low end of the distribution and still is able to cover the wide range of radii used here, 5) $\ln r$ is a natural scale in that the ratio $\Delta r/r$ of interval size to particle size is constant at any point on the axis, and 6) the plot of $g\langle \ln r\rangle$ stays within bounds and still shows the significant aspects of droplet development; other common density functions do not.

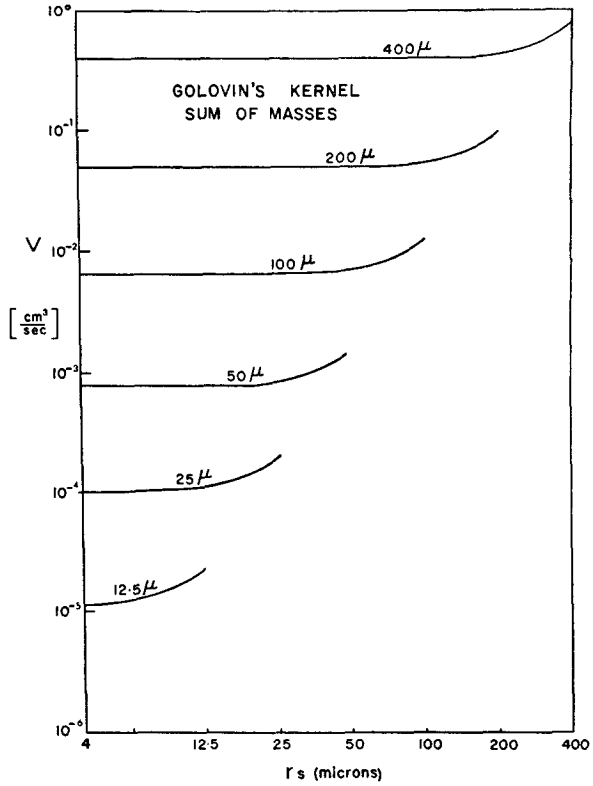

FIG. 2. The collection kernel proportional to the sum of droplet masses (Golovin's kernel).

Let L equal the liquid water content, N the total number of droplets m^{-3}, $\bar{x}_f$ the mean droplet mass (L/N), $s=x/\bar{x}_{f0}$, and the subscript 0 indicate at time zero.

The computations used herein began with the initial density function

$$g\langle \ln r\rangle_0 = 3Ls^2 \exp(-s), \quad (21)$$

for which Golovin (1963) found an analytic solution. It has a mean of $\bar{x}_{g0}=2\bar{x}_{f0}$ and relative dispersion in x of $\sigma_{g0}(x)/\bar{x}_{g0}=2^{-\frac{1}{2}}$. It is equivalent to

$$f\langle \ln r\rangle_0 = 3N_0 s \exp(-s), \quad (21a)$$

which has a mean of $\bar{x}_{f0}=L/N_0$, and a relative dispersion in x of $\sigma_{f0}(x)/\bar{x}_{f0}=1$. In r, the relative dispersion is $\sigma_{f0}(r)/\bar{r}_{f0}=0.364$ which is in the range used by Twomey (1966). In Golovin's form, (21) is

$$f\langle x\rangle = (N_0/\bar{x}_{f0}) \exp(-s). \quad (21b)$$

The radius corresponding to $\bar{x}_{f0}$ is set at 10 μ and L at 1 gm m^{-3}, which gives $N_0=239$ droplets cm^{-3}.

10. Golovin's asymptotic solution

Fig. 2 shows the collection kernel $V=b(x+x')$, for which Golovin (1963) found the complete analytic solution to (21),

$$g\langle \ln r\rangle = 3Ls\tau^{-\frac{1}{2}}(1-\tau)I_1(2\tau^{\frac{1}{2}}s) \exp[-(1+\tau)], \quad (22)$$

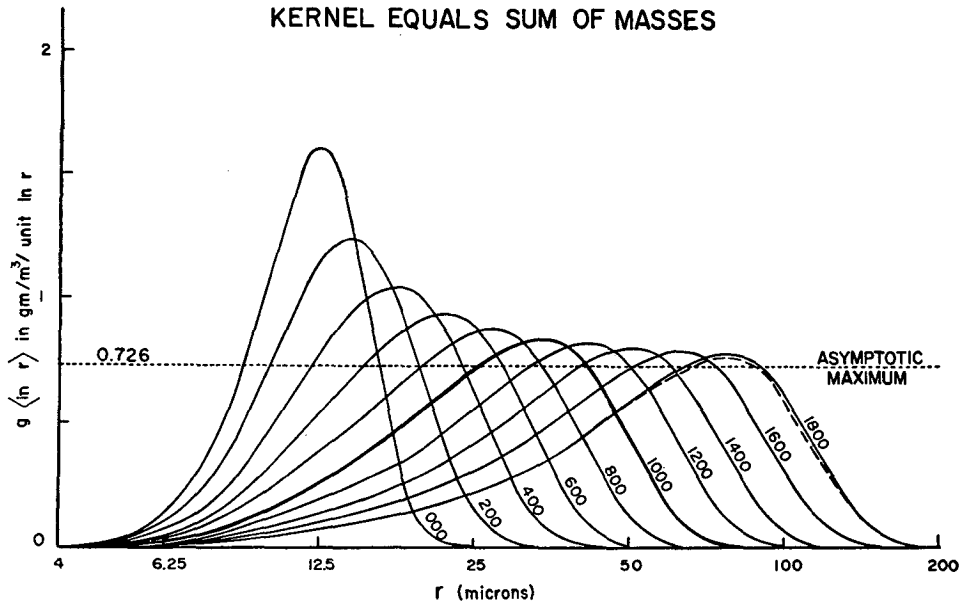

FIG. 3. Computed droplet growth due to the kernel proportional to the sum of droplet masses. The dashed line is Golovin's analytic solution for 1800 sec. The heavy line indicates the growth stage at which Golovin's asymptotic solution becomes a close approximation. The dotted horizontal line at $g\langle\ln r\rangle=0.726$ indicates the maximum $g\langle\ln r\rangle$ of the asymptotic solution.

where

$$\tau=1-\exp(-Lbt),$$

and where I_1 is the modified Bessel function and b a constant. A numerical integration of the collection equation (12) with the above kernel and b equal to 1500 cm^3 gm^{-1} sec^{-1} is shown in Fig. 3, where the time in seconds is shown alongside the individual curves. (The dotted line shows the evaluation of (22) at 1800 sec.)

The asymptotic approximation to (22) is

$$g\langle\ln r\rangle=(3L/2\pi^{\frac{1}{2}})s^{\frac{1}{2}}\exp[-(\tau^{\frac{1}{2}}-1)^2s-Lbt], \quad (23)$$

which is valid for $\tau\approx1$ and $s>1$ [as shown by Scott (1965)]. In Fig. 3, $\tau=0.78$ at $t=1000$ sec, and $\tau=0.95$ at $t=2000$ sec; $s=1$ at $10\,\mu$. The curve $t=1000$ is darkened to indicate that curves for $t\geq1000$ are closely represented by (23) for radii greater than $10\,\mu$. The value of t for a given curve is governed by the magnitude of b, which is arbitrary. But for any b, the curve for $\tau=0.78$ will always be the one that is here labeled 1000 sec. Thus, Golovin's asymptotic approximation is valid in Fig. 3 for curves with the maximum $g\langle\ln r\rangle$ to the right of $35\,\mu$ for radii greater than $10\,\mu$.

The maximum value g_m of $g\langle\ln r\rangle$ and the mode x_m at which it occurs are found from (23) to be

$$g_m=(0.726)L, \quad (24)$$

$$x_m=\bar{x}_{g0}\exp(2Lbt). \quad (25)$$

With (25), (23) may be re-written as

$$g\langle\ln r\rangle=(3L/\pi^{\frac{1}{2}})(x/2x_m)^{\frac{1}{2}}\exp(-x/2x_m), \quad (26)$$

which has the following properties: the mean mass $\bar{x}_g=x_m$ (the mode); the mean square mass is $3^{\frac{1}{2}}x_m$; the variance, $2^{\frac{1}{2}}x_m$; the relative dispersion, $2^{\frac{1}{2}}$. The liquid water content is preserved as shown by

$$\int_1^\infty g\langle\ln r\rangle d\ln r$$

$$=(3L/\pi^{\frac{1}{2}})\int_0^\infty(x/2x_m)^{\frac{1}{2}}\exp(-x/2x_m)dx/3x=L. \quad (27)$$

Thus, the asymptotic $g\langle\ln r\rangle$ is self-preserving.

The radar reflectivity Z of *any* distribution is proportional to the mean mass $\bar{x}_g$ of the mass density function and the total liquid water content. Thus,

$$Z=\int_1^\infty(2r)^6f\langle\ln r\rangle d\ln r$$

$$=(6/\pi\rho)^2L\bar{x}_g, \quad (28)$$

where ρ is the density of water.

Golovin's asymptotic form (26) has

$$(\bar{x}_g/\bar{x}_{g0})=(\bar{x}_f/\bar{x}_{f0})^2. \quad (29)$$

The asymptotic solution in terms of the number density function $f\langle\ln r\rangle$ has no valid mode and a relative dispersion of $\sigma_f(x)/\bar{x}_f=(\bar{x}_g/\bar{x}_f-1)^{\frac{1}{2}}$, which can be shown[6] to be equal to $[2\exp(Lbt)-1]^{\frac{1}{2}}$. Thus, $f\langle\ln r\rangle$ is not self-preserving.

[6] From Scott (1965), $N=N_0\exp(-Lbt)$; so $\bar{x}_f=\bar{x}_{f0}\exp(Lbt)$. Then use (25) and $\bar{x}_{g0}=2\bar{x}_{f0}$.

One's interpretation and insight into particle growth may be tempered by the density function chosen to represent the particle spectrum.

11. Droplet growth for real kernels

The range of real kernels is here represented by geometric sweep-out (Fig. 4), electric field capture (Fig. 7), and hydrodynamic capture (Fig. 9). In addition to the null at $r_s=r$, they differ from Golovin's kernel (Fig. 2), and among themselves, in the derivative, hereafter called the "kernel slope," of $\ln V$ with respect to $\ln r$ or $\ln r_s$, for r or r_s less than 50 μ. This slope change is due partly to the change in the dependence of the terminal velocity on radius from r^2 below 50 μ to r above 50 μ, and partly to Y_c. These kernels were calculated from (1a) using selected constants in a formula for Y_c given in Appendix 1, and the cloud droplet terminal velocities of Gunn and Kinzer (1949) and Mason (1957).

The effect of the null at $r_c=r$ was tested with the kernel $V=b|x-x'|$. This kernel produced a droplet distribution very similar to that for $V=b(x+x')$, but with 0.6 of the growth rate (based upon $\bar{x}_0$).

The growth due to geometric sweep-out ($E_c=1$), shown in Fig. 5, differs from Golovin's form in the initial growth up to 500 sec and by the development of a second maximum at 700 sec.[7] Initially, the primary maximum remains close to its original position near $r=12.5\,\mu$ while the distribution spreads. After the appearance of the second maximum, the form of the density function becomes similar to Golovin's asymptotic solution.

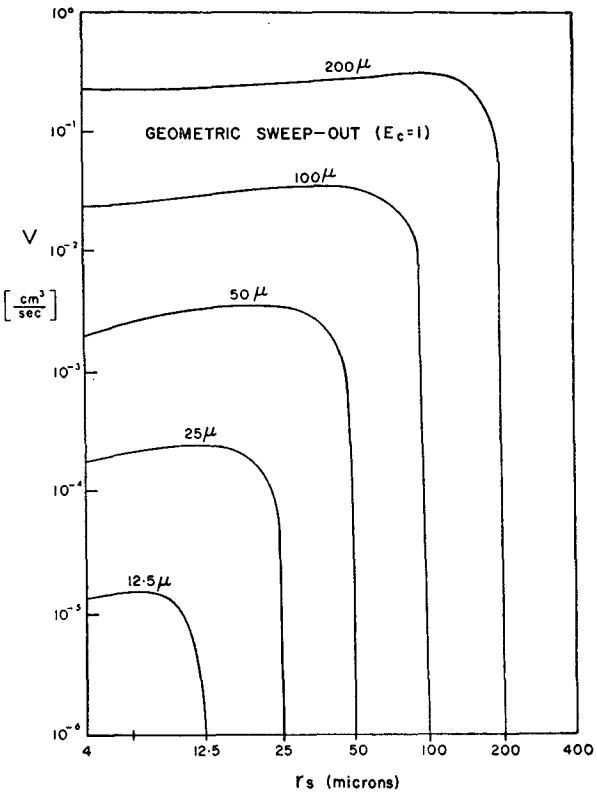

FIG. 4. The collection kernel for geometric sweep-out where $E_c=1$, $Y_c=1+r_s/r$.

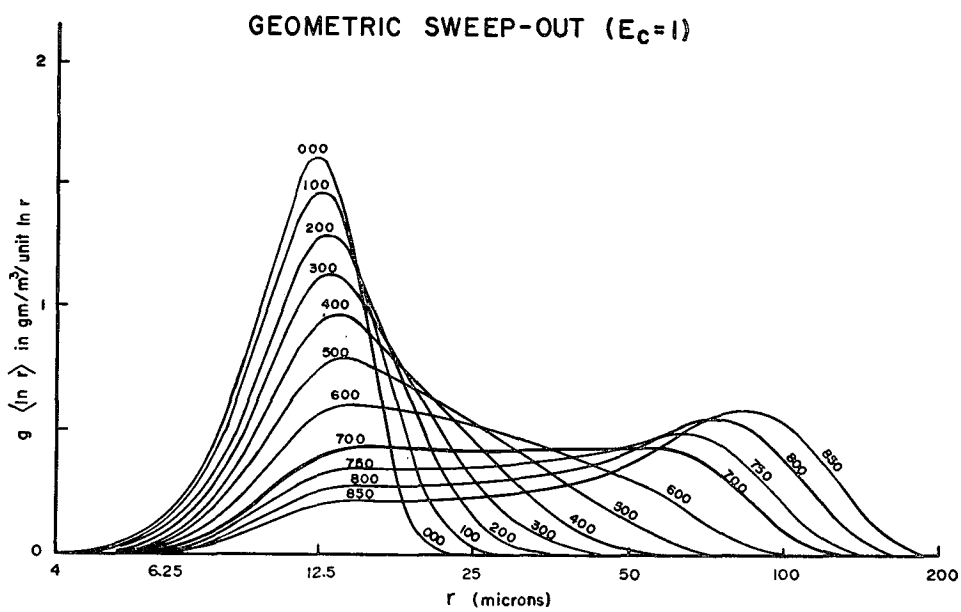

FIG. 5. Computed droplet growth due to geometric sweep-out. The heavy line indicates the appearance of the second maximum.

[7] The second maximum does not occur on the plots of $f\langle\ln r\rangle$. For reference, if $f\langle r\rangle\sim r^{-n}$, then $g\langle\ln r\rangle=rxf\langle r\rangle\sim r^{4-n}$. Thus, the second maximum is where $f\langle r\rangle\sim r^{-4}$.

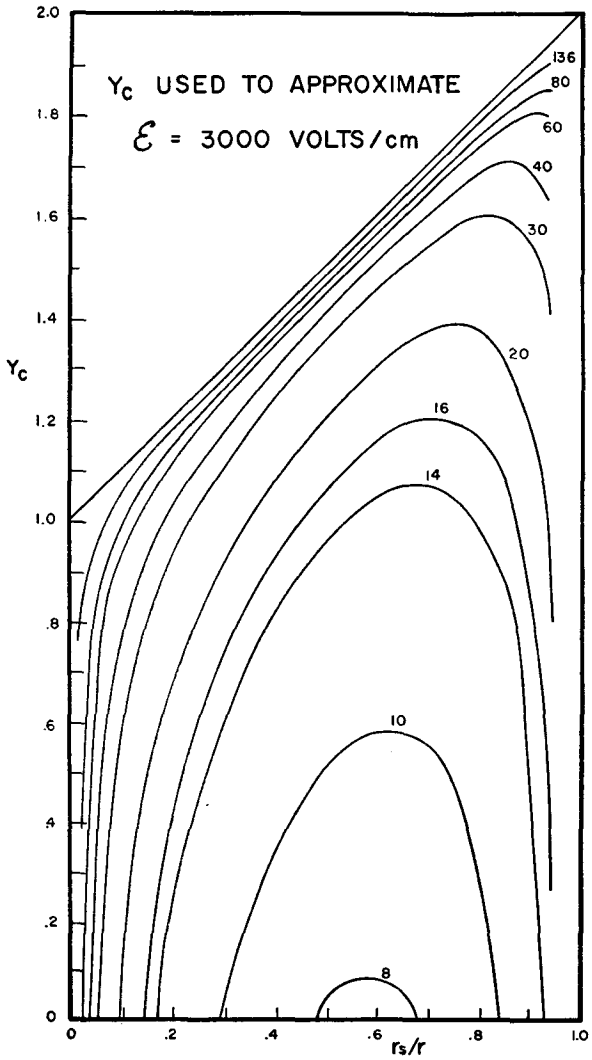

FIG. 6. The linear collection efficiency Y_c used to approximate the values calculated by Plumlee and Semonin (1965) for an electric field of 3000 V cm^{-1}.

Plumlee and Semonin (1965) calculated values of collection efficiency in the presence of an electric field for the radii ranges, $r=30$–$50\,\mu$, $r_s=5$–$15\,\mu$. Since this does not cover the range in radius used here, some extrapolation was necessary to apply their values to these calculations. Their values of E_c at 3000 V cm^{-1} were plotted in terms of Y_c and the constants of Appendix 1 adjusted until a reasonable fit was achieved. The resulting Y_c is shown in Fig. 6. It has a cutoff below $r=8\,\mu$, which may or may not be realistic for droplets in an electric field of this magnitude, and all values of Y_c are below the geometric sweep-out of $Y_c=1+p$. The kernel corresponding to this Y_c is shown in Fig. 7. It differs from Fig. 4 primarily in its greater slope at low r and r_s.

The droplet growth pattern, shown in Fig. 8, for this approximation of the effect of an electric field, differs from geometric sweep-out in that the primary maximum near $12.5\,\mu$ still exists when the secondary maximum at $70\,\mu$ first appears. Also, there is less water in the sizes between 20 and $50\,\mu$ than in Fig. 5. Once the secondary maximum appears, however, it grows rapidly and the density function curve begins to assume a shape similar to Golovin's asymptotic solution. The retainment of the primary maximum is due to the greater slope of V for small droplets than in the case of geometric sweep-out.

The collection kernel for hydrodynamic capture, shown in Fig. 9, was calculated from an analytic formula (given in Appendix 1) that provides a very close approximation to the Y_c values of Shafrir and Neiburger (1963). It differs from the geometric sweep-out in the same general manner as that for the electric field but much more extremely. The cutoff occurs just below $r=18\,\mu$.

The resulting growth, Fig. 10, shows the long time taken (1600 sec) to develop even the smallest amount of water on 100-μ drops. Once this stage has occurred, however, the subsequent accumulation of water on the large droplets is rapid. The primary maximum still exists when the secondary one appears, but it is much higher than in Fig. 8, while the water mass on droplets between 20 and $50\,\mu$ remains extremely small.[8]

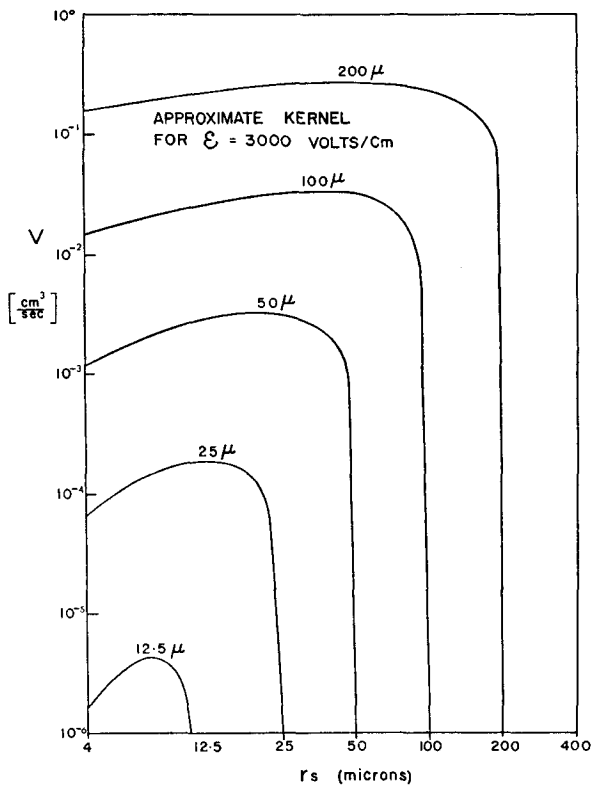

FIG. 7. The collection kernel corresponding to the Y_c of Fig. 6 for the electric field.

[8] Subsequent, more accurate, calculations show that the second maximum of Fig. 10 forms initially near $r=300\,\mu$.

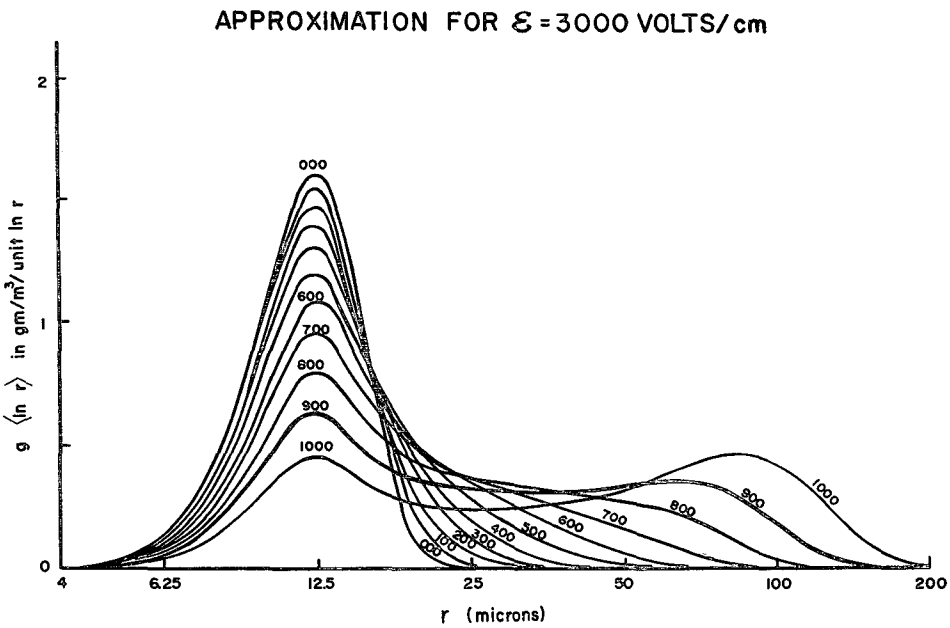

FIG. 8. Computed droplet growth due to the kernel of Fig. 7, approximating the effect of an electric field equal to 3000 V cm^{-1}.

12. A suggested explanation

The patterns of droplet growth and their corresponding kernels suggest the following relationship. There is an "equilibrium" slope on the right hand side of the maximum of $g\langle \ln r \rangle$ that is related to the kernel slope. The greater the kernel slope the less is the equilibrium value of $\partial g\langle \ln r \rangle / \partial \ln r$. This is born out in other calculations, not shown here, with $V=b$ and $V=bxx'$, which result in a very steep slope of $g\langle \ln r \rangle$ for the former and very shallow for the latter.

The exact form of the differentiation of $\ln V$ to obtain the proper "slope" is unclear at this time, but the symmetry $V(r|r_s)=V(r_s|r)$, which follows from the definition of V, must be preserved in the "slope."

This slope V-slope g relationship explains the growth patterns shown here. Fig. 3 shows a constant slope g for a constant slope V. Figs. 5 and 8 show small slope g where slope V is large and the transformation to a larger slope g at large r where slope V is small. This causes a gathering of water mass under a "second maximum." The final slopes of g in Figs. 5 and 8 are similar to the slope g in Fig. 3. For $r>100\,\mu$ their respective kernels are also similar (except for a different b, which only affects the rate of growth and not the form). The growth patterns of Figs. 5, 8 and 10 become similar to Golovin's asymptotic solution because their kernels become similar to $V=b(x+x')$ for $r>60\,\mu$ (neglecting the null at $r_s=r$, which affects the rate more than the form).

Thus, Golovin's asymptotic solution is an approximate asymptotic form for cloud droplet distributions produced by coalescence.

13. Influence of the initial distribution

No other initial distribution was used for these calculations. However, the effect of a narrower initial

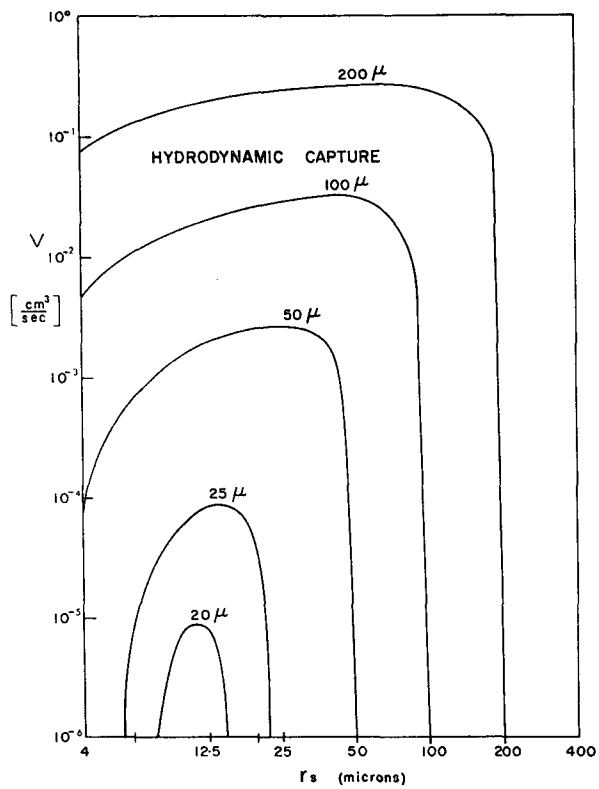

FIG. 9. Kernel for hydrodynamic capture, taken from the values of Y_c calculated by Shafrir and Neiburger (1963).

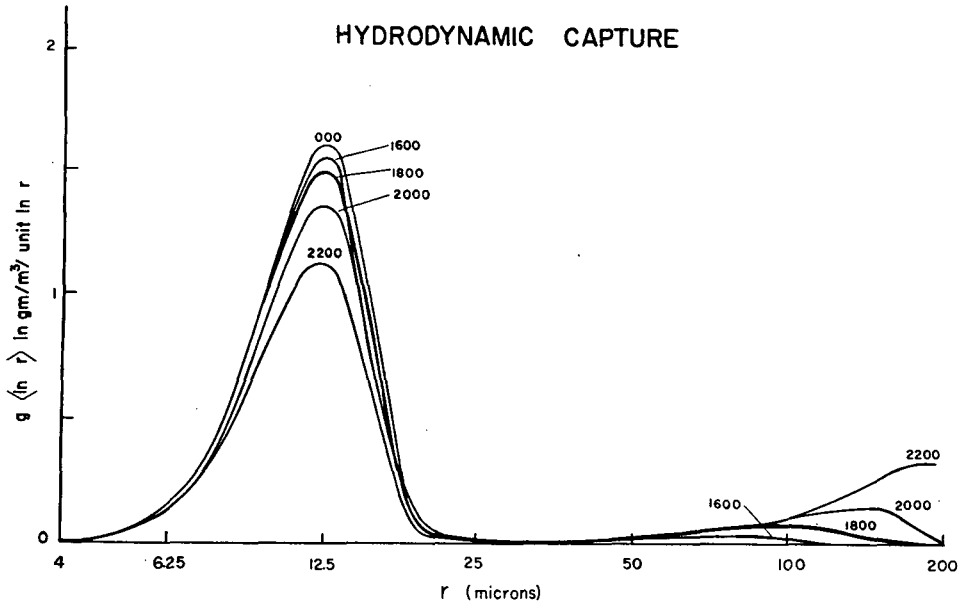

FIG. 10. Computed droplet growth for hydrodynamic capture.

droplet distribution upon Golovin's asymptotic solution may be determined from the solutions of Scott (1965), who solved the sum of masses' problem for the general initial density function, i.e.,

$$f_\nu\langle x\rangle \sim s^\nu \exp[-(\nu+1)s]. \tag{30}$$

The relative variance in x is $(\nu+1)^{-1}$. (We denote the ν-dependent function by the subscript ν.) From Scott's asymptotic solution, we obtain

$$g_\nu\langle \ln r\rangle = (3L/2\pi^{\frac{1}{2}})a^{-\frac{1}{2}}s^{\frac{1}{2}} \exp(-b's - Lbt), \tag{31}$$

where

$$a = (\nu+2)/2(\nu+1),$$
$$b' = (\tau+\nu+1) - (\nu+2)\tau^{1/(\nu+2)},$$

and the mode of $g_\nu\langle \ln r\rangle$ is found to be

$$x_{m\nu} = ax_m', \tag{32}$$

where x_m is given by (25). The mean mass $\bar{x}_{g\nu}$ equals the mode $x_{m\nu}$. The maximum value $g_{m\nu}$ is the same as g_m in (24), $g_\nu\langle \ln r\rangle$ is given by (26) with $x_{m\nu}$ replacing x_m, L is still preserved, and $x_{m\nu}$ replaces x_m in (28). (The smallest coefficient of dispersion used by Twomey (1966) was 0.15 which corresponds to $\nu=4$, $a=\frac{3}{5}$.)

Since (32) is valid at time zero as well as at asymptotic times, $\bar{x}_{g\nu}/\bar{x}_{g\nu 0} = \bar{x}_g/\bar{x}_{g0}$. Thus, the growth rate,

$$\dot{\bar{x}}_{g\nu} = 2Lb\bar{x}_{g\nu}, \tag{33}$$

is independent of ν in (30) for the kernel $V=b(x+x')$. Numerical calculations show that (33) is valid for this kernel at all times, from zero to asymptotic.

The growth rate due to the kernel $V=b|x-x'|$ is also relatively independent of ν for ν as great as 6. For the realistic kernels shown here a narrow distribution will result in slower growth than a wider one, by virtue of having more droplets initially at a size where the "effective b" is very small. The most important property of the initial droplet distribution for growth due to hydrodynamic capture is the amount of water on droplets above the cutoff (18 μ). In the extreme, when all droplets are of a size where $V=0$, no collection can occur at all.

In reality, there may be no droplet size for which $V=0$. The kernels used here neglect the effect of Brownian motion, and Davis (1966) has presented evidence that the theoretical lower cutoff calculated by Hocking (1959) may not be correct, and that instead there may exist no cutoff for gravitational collection.

14. Continuous and stochastic growth

Continuous and stochastic growth are distinguished by the relative amount of water gathered from the various sizes of smaller droplets by large droplets. Droplets growing according to the continuous model gather most of their water by the capture of droplets much smaller than themselves. Droplets growing via the stochastic model gather water from droplets of all smaller sizes. The water mass, and not the number, of droplets captured from each size range is of direct concern; the capture of one large droplet may gather as much water as the capture of one hundred small droplets.

The average rate of mass increase of an r-droplet due to capture of r_s-droplets is equal to the product of the collection kernel (volume swept out per time) and the mass density function (mass per unit volume

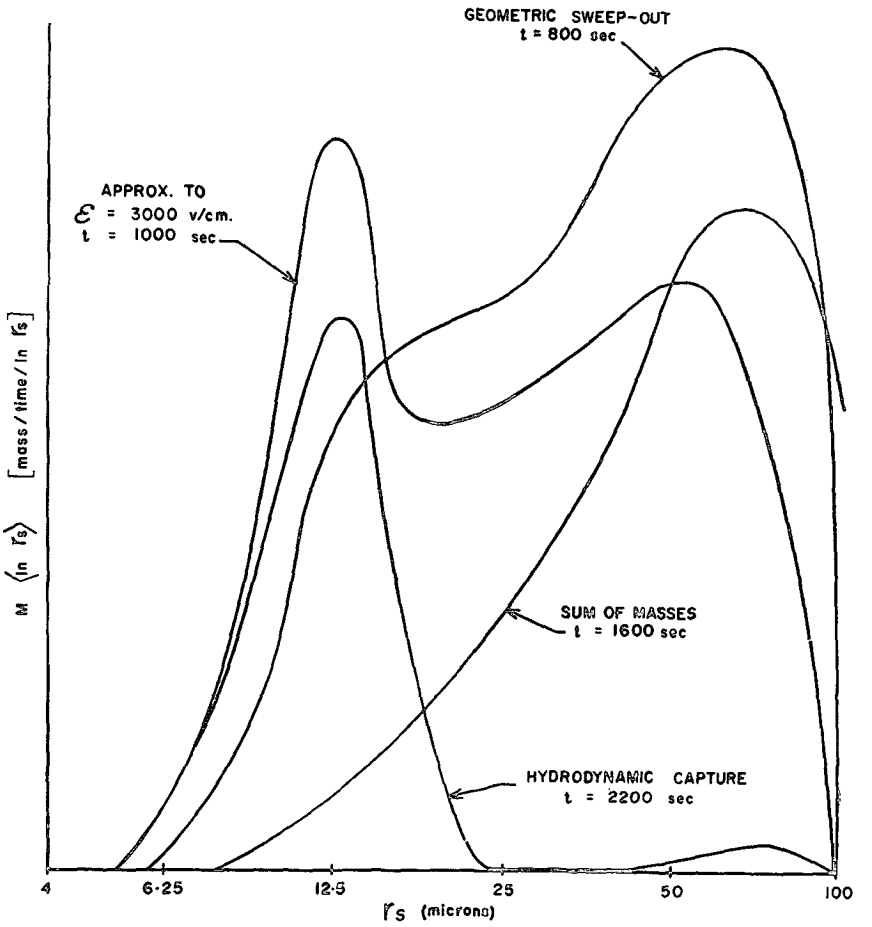

FIG. 11. The relative amount of water mass gathered per unit time by a 100-μ drop from smaller r_s-droplets. Only the shape of the curves is meaningful; the total area under each curve is not.

per unit size interval). This gives the density function

$$M\langle \ln r_s\rangle = V(r|r_s)g\langle \ln r_s\rangle, \tag{34}$$

which is plotted, unnormalized, in Fig. 11 for selected times that correspond to a similar stage of development for each kernel for $r=100\,\mu$. The area under the curve between any two values of r_s is proportional to the rate at which water is gathered by 100-μ drops from r_s-droplets within this size range. (The total area under each curve is here meaningless.)

The stochastic growth equation reduces to the continuous equation when $x \gg x'$ or $r > 2r_s$. In the case of the "sum-of-masses" kernel we see that approximately half the water gathered by 100-μ drops at $t=1600$ sec comes from droplets with $r_s > r/2$. The same would be true of a 50-μ droplet at $t=1000$ sec.

For all kernels the plot of water gathered at $t=0$ by 100-μ drops (of which there are essentially none) is similar to the initial density function. That is, most of the water gathered comes from droplets near 12.5 μ. Thus, a 100-μ drop grows initially according to the continuous model and later according to the stochastic model, as the water mass is gradually shifted to the larger droplets and becomes more available for capture. Fig. 11 shows that growth via geometric sweep-out or a large electric field is quite stochastic after the second maximum forms.

Growth due to hydrodynamic capture is initially continuous but becomes more stochastic as the water mass accumulates under the second maximum. The growth in the region $r=18$–$20\,\mu$ is continuous because the kernel for these sizes is peaked at $r_s=r/2$ and is zero for $r_s \approx r$. Growth between 25—50 μ is continuous because a significant amount of water never accumulates in this region.

The accumulation of water near a given droplet size is governed by the rate of increase of $\ln V$ with $\ln r$ and $\ln r_s$. If $V \sim r^m$, then $\partial \ln V/\partial \ln r = m$, and if $m \geq 4$, water does not accumulate; but if $m=3$, it does. At $r > 60\,\mu$ (where $m \approx 3$), water accumulates under a second maximum and stochastic growth becomes important.

There are several useful methods of comparing the growth rates due to the continuous and stochastic

models. One method is to compare the rate of increase of $\bar{x}_g$. From (25) we see that stochastic growth with the kernel $V=b(x+x')$ gives

$$\dot{\bar{x}}_g=2Lb\bar{x}_g(\text{stochastic}). \tag{35}$$

The continuous growth model, if we assume that the mass of all large droplets is $\bar{x}_g$ and most of the water L is concentrated on smaller droplets, gives $\dot{\bar{x}}_g=VL$. Using the same kernel, with $\bar{x}_g\gg x'$, we get

$$\dot{\bar{x}}=Lb\bar{x}_g(\text{continuous}). \tag{36}$$

Thus, by this comparison, the rate of growth due to the stochastic model is just twice that due to the continuous model. If the kernel $V=b|x-x'|$ were used, the growth rates would be about equal.

The major difference, however, is not in $\bar{x}_g$ but in the amount of water transferred to larger drops. The stochastic model moves the whole liquid water mass with $\bar{x}_g$ to larger droplets, while the continuous model requires that a significant portion of the water be on smaller droplets. Thus, so far as the amount of water mass transferred to larger droplets is concerned, the stochastic model represents a much greater growth rate than the continuous model.

Telford (1955) calculated that the growth rate due to stochastic growth was some 6 times that due to continuous growth. He was, however, not comparing the $\bar{x}_g$'s but the rate of growth of a few larger droplets. He used $E_c=1$, and droplets less than 45 μ, so that $V\sim r^4$.

In Fig. 5 the first 5 min of growth consists of a spread in the distribution with the slope of $g\langle\ln r\rangle$ rapidly decreasing. The initial maximum of $g\langle\ln r\rangle$ moves only slightly. The growth rate of the few largest droplets is at this time much greater than the motion of $\bar{x}_g$. (After 700 sec the opposite is true.)

If we consider at $t=0$ only those droplets with $r>25$ μ, which are present in the quantity of about 10 m^{-3}, and watch them grow (as determined by the numerical output of the calculations), we find that they double their mass every 100 sec. In other words, $\dot{x}$ (stochastic) $=x/50$. On the other hand, continuous growth will take place at the rate $\dot{x}$ (continuous)$=xbL$ and the effective b in this region is $3\cdot10^{-3}$ (m^3 gm^{-1} sec^{-1}), so that $\dot{x}$ (continuous)$=x/300$. Thus, we agree with Telford that $\dot{x}$ (stochastic)$=6\dot{x}$ (continuous) for the few larger droplets at the beginning of collection growth for $r<45$ μ.

15. Summary

1) The mass density function $g\langle\ln r\rangle$ illustrates how the mass of cloud particles (droplets or ice crystals) is distributed over their size when size is plotted logarithmically. It covers a wide range of sizes while showing important detail for small sizes and shows the shift of mass to larger particles during condensation and collection.

2) A narrow initial distribution does not affect the asymptotic form or growth rate for $V=b(x+x')$. If a kernel is very small in the region of the inital water mass, a narrow initial distribution can significantly slow the growth.

3) The equilibrium slope to $g\langle\ln r\rangle$ on the right-hand side of its mode corresponds to the value of m in $V\sim|r\pm r_s|^m$. The greater the value of m the less the slope of $g\langle\ln r\rangle$, and vice versa. The initial spread in the distribution for geometric sweep-out is due to the progress of this slope toward equilibrium. This equilibrium is disturbed above 60 μ where m gradually changes from 4⅓ to 3 and a new equilibrium slope develops.

4) The change in the equilibrium slope of $g\langle\ln r\rangle$ from shallow below 60 μ to steep above 60 μ is responsible for the gathering of water near 100 μ and the consequent formation of the "second maximum."

5) Golovin's solution is an approximate asymptotic form of cloud droplet collection for droplets with radii greater than 60 μ, where $V\sim|r\pm r_s|^3$. Approximately 5 min are needed for droplets above 60 μ to approach this asymptotic form, for $L=1$ gm m^{-3}.

6) This gathering of water makes stochastic collection important.

7) The growth rate due to stochastic collection, using x_m as the standard of comparison and $V=(x+x')$ as the model kernel for the stochastic growth, is just twice that predicted by the continuous model. For $V=b|x-x'|$ the growth rate is about equal. The major difference, however, is that all the water mass moves with the mode in the stochastic model, whereas in the continuous model, most water mass must remain on the small droplets.

Acknowledgments. The author extends thanks to W. A. Mordy for orginally suggesting the pursuit of the coalescence problem, W. T. Scott for a variety of analytic solutions, R. N. Tompson and F. Winterberg for several valuable discussions, and S. Twomey (1966) for a very provocative paper.

APPENDIX

A Formula for Y_c

A general formula for the family of curves of $Y_c(r,p)\geq0$ and $r\geq r_s$ is:

$$Y_c(r,p)=A+Bp+D/p^F+E/(1-p)^G,$$

where

$$p=r_s/r,$$
$$D(r)=D_1/r^{D_2},$$
$$E(r)=E_1/r^{E_2},$$
$$F(r)=(F_1/r)^{M_f}+F_2,$$
$$G(r)=(G_1/r)^{M_g}+G_2+G_3r.$$

The collection efficiencies of Shafrir and Neiburger (1963) are very closely approximated when the above constants take the values: $A=B=1$, $D_1=-27$, $D_2=1.65$, $E_1=-58$, $E_2=1.9$, $F_1=15$, $F_2=1.13$, $G_1=16.7$, $G_2=1$, $G_3=0.004$, $M_f=4$ and $M_g=8$; r is in microns, and negative values of Y_c are set equal to zero.

REFERENCES

Bartlett, J. T., 1966: The growth of cloud droplets by coalescence. Computations of droplet growth for various initial distributions assuming Hocking's values of collection efficiency. *Quart. J. Roy. Meteor. Soc.*, **92**, 93–104.

Berry, E. X, 1965: Cloud droplet growth by collection: a theoretical formulation and numerical calculation. Ph.D. dissertation, University of Nevada. (Available from University Microfilms, Inc., Ann Arbor, Mich.)

Bowen, E. G., 1950: The formation of rain by coalescence. *Australian J. Res.*, **A3**, 193–213.

Braham, R. R., 1964: What is the role of ice in summer showers? *J. Atmos. Sci.*, **21**, 640–645.

Byers, H. R., 1965: *Elements of Cloud Physics*. The University of Chicago Press, 191 pp.

——, and R. K. Hall, 1955: A census of cumulus-cloud height versus precipitation in the vicinity of Puerto Rico during the winter and spring of 1953–1954. *J. Meteor.*, **12**, 176–178.

Chandrasekhar, S., 1943: Stochastic problems in physics and astronomy. *Rev. Mod. Phys.*, **15**, 1–89.

Davis, M. H., 1966: Collisions of very small cloud drops. *J. Geophys. Res.*, **71**, 3101–3104.

Golovin, A. M., 1963: The solution of the coagulation equation for cloud droplets in a rising air current. *Bull. Acad. Sci. USSR*, Geophys. Ser., No. 5, 783–791.

Gunn, R., and G. D. Kinzer, 1949: The terminal velocity of fall for water droplets in stagnant air. *J. Meteor.*, **6**, 243–248.

Handbook on Aerosols, 1950: Atomic Energy Commission, p. 70.

Heywood, G. S. P., 1940: Rain formation in the tropics. *Quart. J. Roy. Meteor. Soc.*, **66**, 46.

Hidy, G. M., 1965: On the theory of the coagulation of non-interacting particles in Brownian motion. *J. Colloid Sci.*, **20**, 123–144.

Hocking, L. M., 1959: The collision efficiency of small drops. *Quart. J. Roy. Meteor. Soc.*, **85**, 44–50.

Howell, W. E., 1949: The growth of cloud drops in uniformly cooled air. *J. Meteor.*, **6**, 134–149.

Huschke, R. E., 1959: *Glossary of Meteorology*. Boston, Amer. Meteor. Soc., 638 pp.

Langmuir, I., 1948: The production of rain by chain reaction in cumulus clouds at temperatures above freezing. *J. Meteor.*, **5**, 175–192.

Mason, B. J., 1957: *The Physics of Clouds*. Oxford University Press, 481 pp.

Melzak, Z. A., 1957: A scalar transport equation. *Trans. Amer. Math. Soc.*, **85**, 547–560.

Mordy, W. A., 1959: Computations of the growth by condensation of a population of cloud droplets. *Tellus*, **11**, 16–44.

——, 1960: Differences in coalescence tendencies in computed condensation cloud droplet spectra. *Physics of Precipitation*, Geophys. Monogr. No. 5, Washington, D. C., Amer. Geophys. Union, 184–190.

——, and L. E. Eber. 1954: Observations of rainfall from warm clouds. *Quart. J. Roy. Meteor. Soc.*, **80**, 48–57.

Neiburger, M., and C. W. Chien, 1960: Computations of the growth of cloud drops by condensation using an electronic digital computer. *Physics of Precipitation*, Geophys. Monogr. No. 5, Washington, D. C., Amer. Geophys. Union, 191–209.

Plumlee, H. R., and R. G. Semonin, 1965: Cloud droplet collision efficiency in electric fields. *Tellus*, **17**, 356–364.

Scott, W. T., 1965: Analytic studies of cloud droplet coalescence. Desert Research Institute, Tech. Rept. No. 9, 36 pp.

——, 1967: Poisson statistics in distributions of coalescing droplets. *J. Atmos. Sci.*, **24**, 221–225.

Shafrir, U., and M. Neiburger, 1963: Collision efficiencies of two spheres falling in a viscious medium. *J. Geophys. Res.*, **68**, 4141–4148.

Smoluchowski, M. V., 1916: Drei Vortrage uber Diffusion, Brownsche Bewegung und Koagulation von Kolloidteilchen. *Phys. Z.*, **17**, 557–585.

Sokolnikoff, I. S., 1951: *Tensor Analysis, Theory and Applications*. New York, John Wiley & Sons, Inc., 335 pp.

Squires, P., 1955: Project Shower: An investigation on warm rain in the Hawaiian Islands. *Nature*, **175**, 748–752.

Telford, J., 1955: A new aspect of coalescence theory. *J. Meteor.*, **12**, 436–444.

Twomey, S., 1964: Statistical effects in the evolution of a distribution of cloud droplets by coalescence. *J. Atmos. Sci.*, **21**, 553–557.

——, 1966: Computations of rain formation by coalescence. *J. Atmos. Sci.*, **23**, 404–411.

Zebel, G., 1958: On the theory of coagulation of electrically uncharged aerosols. *Kolloid Z.*, **156**, 102–107.